The Journal of Fourier Analysis and Applications

"Online First"

Geometric Fourier Analysis for Computational Vision

Jacek Turski

Communicated by D. Healy

ABSTRACT. Projective Fourier analysis—geometric Fourier analysis of the group $\mathbf{SL}(2,\mathbb{C})$*, the group identified in the conformal camera that provides image perspective transformations—is discussed in the framework of representation theory of semisimple Lie groups. The compact model of projective Fourier analysis is constructed, complementing the noncompact model proposed before. Detailed mathematical formulation of both models is presented. It is demonstrated that the projective Fourier analysis provides the data model for efficient perspectively covariant digital image representation well adapted to the retino-cortical mapping of biological visual system, and therefore, explicitly designed for the foveated sensors of a silicon retina, the use of which in active vision systems is presently limited due to the lack of such a model.*

1. Introduction

In computational vision, including machine vision and computational visual neuroscience, image representation should be well adapted to image projective transformations produced by different perspectives between objects and the imaging system. However, computational harmonic analysis, the most sophisticated framework for image representation encompassing models of Fourier, wavelet and Gabor analyses [6, 8, 10, 18], is not well adapted to image perspective transformations. In the search for such an image representation, one is led to the aspects of harmonic analysis associated with abstract procedure in group theory—unitary group representations, and in particular, geometric Fourier analysis. In this framework, the generalized Fourier transform plays the same role on any group, as the classical Fourier transform on the additive group of real numbers, where the irreducible unitary representations are homomorphisms between this group and the multiplicative group of complex numbers of modulus one (the circle group). Since group theory is rooted in large part in geometry through Klein's Erlanger Program of studying spaces through their groups of

Math Subject Classifications. 43A30, 43A65, 43A85, 68T10, 68U10.
Keywords and Phrases. The conformal camera, representation theory of semisimple Lie groups, geometric Fourier analysis, perspectively adapted image processing, retinotopic mapping, foveated vision.
Acknowledgments and Notes. This work is supported in part by NSF grant CCR-9901957.

ISSN 1069-5869 DOI: 10.1007/s00041-004-0972-x

motions, this geometric Fourier analysis emphasizes from the very beginning the covariance with respect to the geometric transformations. The above mentioned Fourier, wavelet and Gabor analyses involve irreducible unitary representations of Euclidean, affine and Weyl-Heisenberg groups, or subgroups, and therefore, they are not well adapted to image perspective transformations.

In computational neuroscience of the brain's visual pathway [15], the image representation should be also well adapted to the visuotopic (retinotopic, or topographic) mapping—the mapping that provides the initial stage in the process by which the brain processes visual information. In this processing stage, the visual field is centrally projected onto the retina of the eye where it is sampled by nonuniformly distributed light-sensitive cells with the highest density at the fovea and concentrically decreasing toward the periphery. This retinal image is carried by the optic nerve to the lateral geniculate nucleus (LGN) of the thalamus, where most of the axons must synapse. From there, the visual information is relayed via optic radiation and ultimately arrives as a cortical image to the primary visual cortex, which has a constant density of neural cells and is located on the back of the brain. The topographic arrangement of axons along the visual pathway with the difference in the densities of cells in the retina and the visual cortex, produces a highly distorted cortical image of the visual field. In biologically motivated machine vision systems [22], consisting of the digital camera with a retina-like sensor architecture (silicon retina), coupled with a hardware image processor and linked to a computer performing image analysis, the silicon retina and image processor produce the digital image similar to the cortical image of the retinotopic mapping. In spite of the advantages such as data processing reduction and similarity invariance, the use of the silicon retina architecture in active vision systems is presently limited due to the lack of elegant image processing tools [31].

The image representation well adapted to image projective transformations has been proposed and studied in a series of articles: [26, 27, 28, 29]. It has been done by constructing projective Fourier analysis of the conformal camera. In this camera, the semisimple Lie group $\mathbf{SL}(2,\mathbb{C})$, acting by linear-fractional mappings on the complex image plane, provides the image projective transformations consisting of image perspective transformations and conformal distortions resulting from the "conformal lens optics" of the camera [28]. In this analysis, an image is decomposed in terms of the one-dimensional irreducible unitary representations of the Borel subgroup of $\mathbf{SL}(2,\mathbb{C})$, with the coefficients of the representations given by projective Fourier transform. Using this decomposition, we could render pattern's projective transformations by computing only one projective Fourier transform of the original pattern. Feasibility of this projective characteristic of the data model rests on the following fact: Although, all nontrivial unitary representations of the group $\mathbf{SL}(2,\mathbb{C})$ are infinite-dimensional, all finite-dimensional irreducible unitary representations of the Borel subgroup are one-dimensional, and this subgroup exhausts the "projective" part of $\mathbf{SL}(2,\mathbb{C})$.

In this article, we present the "whole" projective Fourier analysis and also demonstrate that it provides the computational framework well suited for developing efficient image processing tools explicitly designed for foveated vision systems, both biological and artificial. In the framework of geometric Fourier analysis of the semisimple Lie groups, we construct the two models of the projective Fourier analysis. The first one (proposed in [26]) is based on the noncompact picture of the induced unitary representations of $\mathbf{SL}(2,\mathbb{C})$, while the second one involves the (reduced) compact picture of such representations. Both pictures have been used to study representations of semisimple Lie groups [17]. Further, after we review the derivation of the discrete projective Fourier transform in the noncompact model, analytical aspects of the data model for digital image representation based on it are

discussed. In particular, we show how to correct the conformal lens optics of the camera in order to render digital image perspective transformations. The projective Fourier transform when expressed in log-polar coordinates (by identifying $\ln re^{i\theta} = \ln r + i\theta$ with $(\ln r, \theta)$), becomes the standard Fourier transform. Thus, in the log-polar coordinates plane, we can compute efficiently the discrete projective Fourier transform of an image by applying a 2-D FFT. It has been evidenced in experimental neuroscience that the retinotopic mapping of the visual field to the primary visual cortex in primates, is characterized by a complex logarithmic transformation [23]. Therefore, the projectively covariant digital image representation developed in this work, is well adapted to both the retinotopic mapping of the brain visual pathway and the silicon retina sensors of active vision systems. This aspect of projective Fourier analysis was presented by the author on the SIAM conference [30]; see also the article by James Case in the December 2003 issue of SIAM News.

Fourier analysis on groups, their homogeneous spaces, and on symmetric spaces in particular, based on geometric ideas was originated by Gelfand's school and Harish-Chandra, and further developed by Helgason [11]. Although, we work with geometric Fourier analysis of $\mathbf{SL}(2, \mathbb{C})$, harmonic analysis for the simplest noncompact semisimple complex Lie group (developed by Gelfand's school [9]), it is advantageous to discuss the projective Fourier analysis in a more general context of semisimple Lie groups (Harish-Chandra's approach). A good introduction to the field of representation theory of semisimple Lie groups can be found in [17]. However, the reader who is not familiar with the basic definitions and facts of representation theory of semisimple Lie groups (including the definition of a semisimple Lie group in the context used in this article) is referred to [14], where an elementary account of Harish-Chandra's fundamental (but very technical) work in the field of representation theory is also given.

2. The Group of Image Projective Transformations

2.1 The Conformal Camera

The camera model is based on the perspective projection

$$j(x_1, x_2, x_3) = \frac{x_3 + ix_1}{x_2} \,. \tag{2.1}$$

Thus, the space points are centrally projected through the origin on the image plane $x_2 = 1$ where the points $(x_1, 1, x_3)$ are identified with complex numbers $x_3 + ix_1$. Next, the projection is embedded into the complex plane

$$\mathbb{C}^2 = \left\{ \begin{pmatrix} z_1 \\ z_2 \end{pmatrix} \mid z_1 = x_2 + iy, z_2 = x_3 + ix_1 \right\}$$

such that the complex line $z_2 = \xi z_1$ of "slope" ξ satisfying $y = 0$ corresponds to the line in $\mathbb{R}^3$ that passes through the origin and intersects the image plane $x_2 = 1$ at the point $\xi = x_3 + ix_1$. One assumes that the line $z_1 = 0$ has the slope ∞, and regards the image plane as the extended complex line $\widehat{\mathbb{C}} = \mathbb{C} \cup \{\infty\}$ where $j(x_1, 0, x_3) = \infty$. The action of the Lie group $\mathbf{SL}(2, \mathbb{C})$ on nonzero column vectors $\binom{z_1}{z_2}$ in $\mathbb{C}^2$ induces the action on the slopes of all complex lines through the origin in $\mathbb{C}^2$ by the linear-fractional transformations:

If $g = \left(\begin{smallmatrix} \alpha & \beta \\ \gamma & \delta \end{smallmatrix}\right)$ then

$$\xi \longmapsto g \cdot \xi = \frac{\delta\xi + \gamma}{\beta\xi + \alpha} \,. \tag{2.2}$$

The action (2.2) gives the image transformations of patterns, or planar objects viz.: If $f : D \to \mathbb{R}$ is the intensity function of a pattern, then $f_g : gD \to \mathbb{R}$, defined by $f_g(z) = f(g^{-1} \cdot z)$, is the intensity function of the transformed pattern under the action of $g \in \mathbf{PSL}(2, \mathbb{C}) = \mathbf{SL}(2, \mathbb{C})/\{\pm I\}$. The camera possesses the "conformal lens optics" because the linear-fractional transformations in (2.2) are conformal mappings, and therefore, it is referred to as the *conformal camera.* It is described in Section 2.3 in physical terms and its usefulness in computational vision is discussed in Section 2.4.

2.2 Geometry of the Image Plane

The image plane $\widehat{\mathbb{C}}$ of the conformal camera can be dually identified either with:
(1) The complex projective line $P^1(\mathbb{C})$ where

$$P^1(\mathbb{C}) = \left\{\text{complex lines in } \mathbb{C}^2 \text{ through the origin}\right\} .$$

The projective geometry of $\mathbb{C}$ is describe by the group of projective transformations $\mathbf{PSL}(2, \mathbb{C}) = \mathbf{SL}(2, \mathbb{C})/\{\pm I\}$, see [3], or with

(2) The Riemann sphere where the isomorphism $\widehat{\mathbb{C}} \cong S^2_{(0,1,0)}$ is given by stereographic projection [cf. (2.1)]

$$j|_{S^2_{(0,1,0)}} : S^2_{(0,1,0)} \to \widehat{\mathbb{C}} \,. \tag{2.3}$$

The group $\mathbf{PSL}(2, \mathbb{C})$ acting on $\widehat{\mathbb{C}}$ consists of the group of automorphisms [16] that preserve the intrinsic geometry imposed by complex structure, known as *Möbius geometry* [12], or *inversive geometry* [4].

2.3 Image Projective and Perspective Transformations

The maximal compact subgroup $\mathbf{SU}(2) = \left\{\left(\begin{smallmatrix} \alpha & \beta \\ -\overline{\beta} & \overline{\alpha} \end{smallmatrix}\right) \mid |\alpha|^2 + |\beta|^2 = 1\right\}$ in $\mathbf{SL}(2, \mathbb{C})$ is the universal double covering group of the group of rotations $\mathbf{SO}(3)$, [5]. To express this relation, the elements $R \in \mathbf{SO}(3)$ rotating the sphere $S^2_{(0,1,0)}$ about its center $(0, 1, 0)$ (cf., Section 5.2), are parametrized by the Euler angles (ψ, ϕ, ψ') where ψ is the rotation angle about the x_2-axis, followed by the rotation angle ϕ about the x_3'-axis that is parallel to the x_3-axis and passing through $(0, 1, 0)$, and finally by the rotation angle ψ' about the rotated x_2-axis. Then under the covering, to each $R(\psi, \phi, \psi')$ in $\mathbf{SO}(3)$ there correspond two elements in $\mathbf{SU}(2)$,

$$k\big(\psi, \phi, \psi'\big) = \pm \begin{pmatrix} e^{i\psi/2} & 0 \\ 0 & e^{-i\psi/2} \end{pmatrix} \begin{pmatrix} \cos\frac{\phi}{2} & i\sin\frac{\phi}{2} \\ i\sin\frac{\phi}{2} & \cos\frac{\phi}{2} \end{pmatrix} \begin{pmatrix} e^{i\psi'/2} & 0 \\ 0 & e^{-i\psi'/2} \end{pmatrix} , \tag{2.4}$$

acting on $\mathbb{C}$ as in (2.2), such that

$$j|_{S^2_{(0,1,0)}} \circ R\left(\psi, \phi, \psi'\right) = k\left(\psi, \phi, \psi'\right) \circ j|_{S^2_{(0,1,0)}} \,. \tag{2.5}$$

For translations, if $(x_1, 1, x_3)$ is translated by the vector $t = (t_1, t_2, t_3)^t \in \mathbb{R}^3$ such that $t_2 \neq -1$ and projected back to the image plane by (2.1), we get $(x_3 + ix_1 + t_3 + it_1)/(1 + t_2) = \left(\alpha^{-1}\xi + \beta\right)/\alpha$ where $\alpha = (1 + t_2)^{1/2}$, if $1 + t_2 > 0$, $\alpha = i\,(|1 + t_2|)^{1/2}$, if $1 + t_2 < 0$, and $\beta = \gamma\alpha^{-1}$ with $\gamma = (t_3 + it_1)$. Therefore, there are two elements in $\mathbf{SL}(2, \mathbb{C})$,

$$h(t_1, t_2, t_3) = \pm\begin{pmatrix} \alpha & 0 \\ \beta & \alpha^{-1} \end{pmatrix} = \pm\begin{pmatrix} \alpha & 0 \\ 0 & \alpha^{-1} \end{pmatrix}\begin{pmatrix} 1 & 0 \\ \gamma & 1 \end{pmatrix},$$

such that

$$j \circ t = h(t_1, t_2, t_3) \circ j|_{S^2_{(0,1,0)}}\,. \tag{2.6}$$

It implies the factorization of h: If $1 + t_2 > 0$, then $h \in \mathbf{A}\widetilde{\mathbf{N}}$, and, if $1 + t_2 < 0$, then $h = \varepsilon\mathbf{A}\widetilde{\mathbf{N}}$, $\varepsilon = \left(\begin{smallmatrix} -i & 0 \\ 0 & i \end{smallmatrix}\right)$, where $\widetilde{\mathbf{N}} = \left\{\left(\begin{smallmatrix} 1 & 0 \\ \gamma & 1 \end{smallmatrix}\right) \mid \gamma \in \mathbb{C}\right\}$, and $\mathbf{A} = \left\{\left(\begin{smallmatrix} \delta & 0 \\ 0 & \delta^{-1} \end{smallmatrix}\right) \mid \delta \in \mathbb{R}_+\right\}$ are the closed subgroups of $\mathbf{SL}(2, \mathbb{C})$.

From (2.5) and (2.6) emerges description of the conformal camera in physical terms: Patterns as two-dimensional entities "live" on the image plane and their projective transformations are generated by: (i) projecting the pattern into the sphere $S^2_{(0,1,0)}$, rotating the sphere by $R(\psi, \phi, \psi')$, and, then projecting the rotated pattern back to the image plane; the resulting image projective transformation $z' = k(\psi, \phi, \psi') \cdot z$ [see Figure 1 (A)], and (ii) translating the pattern out of the image plane by a vector $t = (t_1, t_2, t_3)^t$, and, then projecting it back to the image plane; the resulting image projective transformation $z' = h(t_1, t_2, t_3) \cdot z$ [see Figure 1 (A)].

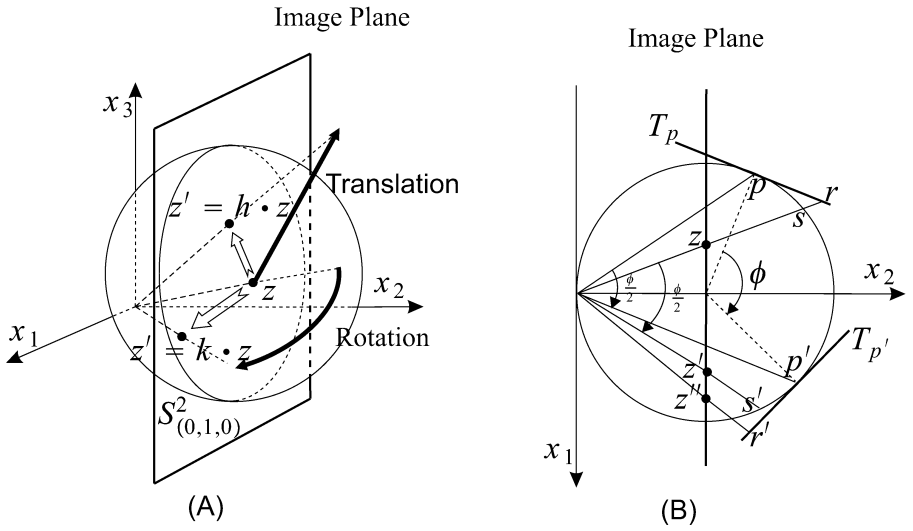

FIGURE 1 (A) The image projective transformations in the conformal camera are generated by rotations and translations. (B) The deconformalization process; for convenience only the intersection of the conformal camera with the plane $x_3 = 0$ is shown.

It follows from the polar (or **KAK**) decomposition $\mathbf{SL}(2,\mathbb{C}) = \mathbf{SU}(2)\mathbf{ASU}(2)$, [17], that the finite iterations of the basic image projective transformations given by $\mathbf{SU}(2)$ and $\mathbf{A}$ generate the group of image projective transformations $\mathbf{SL}(2,\mathbb{C})$.

In order to obtain the image perspective transformations, its projective transformations under the action of (2.4) need the correction for conformal distortions. It is done as follows, see Figure 1 (B). We choose a point $\eta = b + ia$ of the pattern and extend its projection from the sphere $S^2_{(0,1,0)}$ to the plane T_p tangent to the sphere at the point $p = \sigma(\eta) = \left(a^2 + b^2 + 1\right)^{-1}(2a, 2, 2b)$ where σ is the inverse of stereographic projection (2.3). After rotating the sphere $S^2_{(0,1,0)}$ (with the tangent plane T_p attached to it) about the x_3'-axis by the angle $-\phi$ (for simplicity, $\psi = \psi' = 0$), and projecting it back from the (rotated) tangent plane, we obtain the projective transformations corrected for conformal distortions; that is, the perspective transformations. We refer to it as *deconformalization of the image projective transformations.*

Explicitly, the real and imaginary parts of the coordinates $z' = x_3' + ix_1'$, of the projective transformations $z' = k(0, -\phi, 0)\cdot z$,

$$\begin{aligned} x_3' &= \frac{2x_3}{\left(x_1^2 + x_3^2\right)(1-\cos\phi) + 2x_1\sin\phi + \cos\phi + 1} \\ x_1' &= \frac{\left(x_1^2 + x_3^2\right)\sin\phi + 2x_1\cos\phi - \sin\phi}{\left(x_1^2 + x_3^2\right)(1-\cos\phi) + 2x_1\sin\phi + \cos\phi + 1}\,. \end{aligned} \tag{2.7}$$

include conformal distortions (we took $-\phi$ because $k(0, -\phi, 0)$ maps the pattern form the first quadrant into this quadrant). Then, the corresponding coordinates $z'' = x_3'' + ix_1''$ of the perspective transformation (with chosen $\eta = b + ia$) are given by

$$\begin{aligned} x_3'' &= \frac{2x_3}{\left(2ax_1 - a^2 + 2bx_3 - b^2\right)(1-\cos\phi) + 2x_1\sin\phi + \cos\phi + 1} \\ x_1'' &= \frac{\left(2ax_1 - a^2 + 2bx_3 - b^2\right)\sin\phi + 2x_1\cos\phi - \sin\phi}{\left(2ax_1 - a^2 + 2bx_3 - b^2\right)(1-\cos\phi) + 2x_1\sin\phi + \cos\phi + 1}\,. \end{aligned} \tag{2.8}$$

The extension to general image projective transformations is straightforward.

We can see in Figure 2 (A) the image projective transformation of a single vertical bar [shown in Section 6.2 in Figure 3 (A)] under (2.7) with $\phi = 30°$ and in Figure 2 (B) the image corrected for conformal distortions by using (2.8).

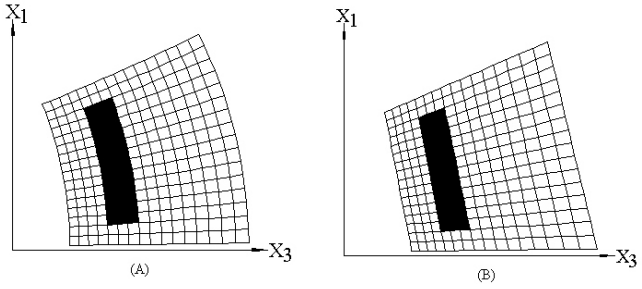

FIGURE 2 Correcting the conformal lens optics of the camera.

2.4 The Conformal Camera and Computational Vision

The cameras used in machine vision, including the most common pinhole camera, involve 3×4 real matrices describing the composed effect of the projection of the space points on the image plane and the corresponding transformations between the space and the image plane coordinates. See [25] for their classifications in terms of the corresponding 3×4 matrices. These cameras are used to extract geometric information from scenes, such as projective invariants [19], and based on this information, to acquire a 3-D understanding of the scenes. However, the set of 3×4 matrices describing a particular camera does not form a group, which is a major obstacle in developing a group theoretical approach to image representation that is well adapted to image transformations produced by the camera. On the other hand, the conformal camera as introduced and discussed in the previous parts of this section, is characterized by the image projective transformations given by the action of the group $\mathbf{SL}(2, \mathbb{C})$ on the points of the image plane. This group action has a well understood harmonic analysis, a sophisticated computational framework for developing projectively adapted image processing tools. In particular, the conformal camera is formulated for planar images, or patterns and most of man made objects contain identifiable piece of a planar surface which is enough to use the projective convolutions to recognize 3-D objects in dynamic scenes.

Despite the fact demonstrated later in Section 6, that the projective Fourier analysis based on the conformal camera, provides image processing tools for digital cameras with the human-like visual sensor architecture (Section 6.2), (DPFT and biologically motivated machine vision), the conformal camera is less intuitive than cameras that have been used in computer vision. However, it passes the following fundamental property: It *reduces* the degrees of freedom by identifying those perspective transformations for which different objects have the same perspective projection. It can be understood from Figure 1 (A) by examining how image projective transformations are generated and extending the projecting rays into the visual field on the left of the camera. Further, those remaining degrees of freedom are the once that are relevant for the biological visual systems. It follows from the observation that such systems employ mostly different strategies than the purely geometric strategies that use, say, projective invariants, in gaining the understanding the 3-D word from 2-D images.

More precisely, if we examine a biological visual system such as the human visual system, we realize that the eye (the camera with almost spherical image surface) does not "see" the visual field that is centrally projected on its retina, as it contains photoreceptor cells with chemicals that release energy when struck by light. The ganglion cells of the retina, after pre-processing the retinal image, transmit the visual information (variation in released energy) by way of the optic nerve to the lateral geniculate nucleus (LGN) of the thalamus. From there, the LGN axons fan out further it through the deep white matter of the brain as the optic radiations to the primary visual cortex, an area in the visual cortex on the back of the brain. The highly structured topographic arrangement of axons along the visual pathway (called the retinotopic mapping) with the nonuniform distribution of photoreceptors in the retina with the highest density at the fovea which decreases toward the periphery, on one hand side, and a constant density of neural cells in the visual cortex, on the other, produce the cortical image showing a dramatic distortion of the visual field with a significant magnification of the foveal region. The brain processes this visual information by dividing and sending it further along two streams: (1) a medial, "Action," or "Where" stream which is concerned with the spatial relationship between objects for the unconscious

guidance movement and, (2) a lateral "What" stream which is concerned conscious object recognition and perception. The Action/Where stream gets its input from the periphery retina. However, it is the What stream that gets its input primarily from the foveal region and (among many other things, not all fully understood) extracts many visual cues about the 3-D word from 2-D images, such as the depth cues from binocular disparity and monocular motion parallax, and "sees" the coherent image [15].

It has been evidenced by Eric Schwartz in [23] that the retinotopic mapping can be described by a complex logarithm. Subsequently he proposed different logarithmic functions, notably $\ln(z+a)$ and $\ln((z+a)/(z+b))$. However, the retinotopic mapping varies across species and therefore, to model the aspects of peripheral vision with the correct cortical magnification of the foveal region, it could be represented simply by $\ln z$. It follows that rotations and scale changes of a pattern correspond under the retinotopic mapping to the cortical translations viz.: $\ln\left(\rho e^{i\alpha} r e^{i\theta}\right)$ corresponds to $(\ln r + \ln\rho, \theta+\alpha)$. In the visual pathway without the retinotopic mapping, the brain must have much bigger size (at least 5000 lb. by Schwartz estimate [24]) in order to process all the visual information reaching the eye.

Using the projective Fourier analysis constructed in Section 5, we demonstrate later in Section 6, that the digital data model developed upon harmonic analysis of the conformal camera provides the efficient computational framework for the initial stage by which the brain processes visual information that is carried from the retina of the eye to the primary visual cortex. This follows from the fact that in log-polar coordinates $(\ln r, \theta)$ (identified with the principal complex logarithm $\ln z = \ln\left(re^{i\theta}\right) = \ln r + i\theta$), the projective Fourier transform of a pattern takes on the standard Fourier integral form, and therefore, it can be computed efficiently by 2-D FFT. In order to apply FFT, the pattern must be re-sampled with nonuniform log-polar sampling geometry (pixels of retinal image) and expressed in the log-polar coordinate plane with uniform (rectangular) sampling geometry (pixels of cortical image), see [30].

3. Analysis on $\mathbf{SL}(2,\mathbb{C})$

Both Iwasawa and Gauss decompositions of semisimple Lie groups play important roles in the construction of induced representations of such groups in general, and of the group $\mathbf{SL}(2,\mathbb{C})$ in particular. To this end, in addition to the subgroups $\mathbf{SU}(2)$, $\mathbf{A}$, and $\widetilde{\mathbf{N}}$, we also need the subgroup $\mathbf{N} = \left\{\left(\begin{smallmatrix}1 & \gamma\\ 0 & 1\end{smallmatrix}\right) \mid \gamma\in\mathbb{C}\right\}$.

3.1 Iwasawa Decomposition

We want to write any $g = \left(\begin{smallmatrix}\alpha & \beta\\ \gamma & \delta\end{smallmatrix}\right) \in \mathbf{SL}(2,\mathbb{C})$ in the form $g = \mathrm{kan}$ with $k\in\mathbf{SU}(2)$, $a\in\mathbf{A}$ and $n\in\mathbf{N}$. This is given as follows:

$$g = \begin{pmatrix} \frac{\alpha}{\sqrt{|\alpha|^2+|\gamma|^2}} & \frac{-\overline{\gamma}}{\sqrt{|\alpha|^2+|\gamma|^2}} \\ \frac{\gamma}{\sqrt{|\alpha|^2+|\gamma|^2}} & \frac{\overline{\alpha}}{\sqrt{|\alpha|^2+|\gamma|^2}} \end{pmatrix} \begin{pmatrix} \sqrt{|\alpha|^2+|\gamma|^2} & 0 \\ 0 & \frac{1}{\sqrt{|\alpha|^2+|\gamma|^2}} \end{pmatrix} \begin{pmatrix} 1 & \frac{\overline{\alpha}\beta+\overline{\gamma}\delta}{|\alpha|^2+|\gamma|^2} \\ 0 & 1 \end{pmatrix}, \quad (3.1)$$

which shows its uniqueness. Further, we see from (3.1) that the multiplication map

$$\mathbf{SU}(2)\times\mathbf{A}\times\mathbf{N}\to\mathbf{SL}(2,\mathbb{C}), \quad (k,a,n)\mapsto \mathrm{kan}$$

is a diffeomorphism onto.

The decomposition $\mathbf{SL}(2,\mathbb{C}) = \mathbf{SU}(2)\mathbf{AN}$ is called the *Iwasawa decomposition* of $\mathbf{SL}(2,\mathbb{C})$. If $g \in \mathbf{SL}(2,\mathbb{C})$ decomposes under $\mathbf{SU}(2)\mathbf{AN}$, we write $g = k(g)a'(g)n$.

3.2 Gauss Decomposition

For each element $g = \left(\begin{smallmatrix}\alpha & \beta\\ \gamma & \delta\end{smallmatrix}\right) \in \mathbf{SL}(2,\mathbb{C})$ we have one of the two cases: $\alpha \neq 0$, or $\alpha = 0$. If $\alpha \neq 0$, then we can write $g = \left(\begin{smallmatrix}1 & 0\\ \gamma/\alpha & 1\end{smallmatrix}\right)\left(\begin{smallmatrix}\alpha & \beta\\ 0 & \alpha^{-1}\end{smallmatrix}\right)$ where we used that $\alpha\delta - \beta\gamma = 1$. If $\alpha = 0$, then $g = \left(\begin{smallmatrix}0 & 1\\ -1 & 0\end{smallmatrix}\right)\left(\begin{smallmatrix}\beta^{-1} & -\delta\\ 0 & \beta\end{smallmatrix}\right)$. Then introducing the Borel subgroup $\mathbf{B} = \left\{\left(\begin{smallmatrix}\alpha & \beta\\ \mathbf{0} & \alpha^{-1}\end{smallmatrix}\right) \mid \alpha \in \mathbb{C}_*, \beta \in \mathbb{C}\right\}$ of $\mathbf{SL}(2,\mathbb{C})$, we can write that for any $g \in \mathbf{SL}(2,\mathbb{C})$ either $g \in \widetilde{\mathbf{N}}\mathbf{B}$, or $g \in p\mathbf{B}$ where $p = \left(\begin{smallmatrix}0 & 1\\ -1 & 0\end{smallmatrix}\right)$. Thus,

$$\mathbf{SL}(2,\mathbb{C}) = \widetilde{\mathbf{N}}\mathbf{B} \cup p\mathbf{B}\,. \tag{3.2}$$

Further, since

$$b = \begin{pmatrix}\alpha & \beta\\ 0 & \alpha^{-1}\end{pmatrix} = \begin{pmatrix}\frac{\alpha}{|\alpha|} & 0\\ 0 & \frac{|\alpha|}{\alpha}\end{pmatrix}\begin{pmatrix}|\alpha| & 0\\ 0 & \frac{1}{|\alpha|}\end{pmatrix}\begin{pmatrix}1 & \frac{\beta}{\alpha}\\ 0 & 1\end{pmatrix}, \tag{3.3}$$

we see that the Borel subgroup $\mathbf{B}$ factors as $\mathbf{B} = \mathbf{MAN}$, with both $\mathbf{N}$ and $\mathbf{AN}$ normal in $\mathbf{B}$. Using it and (3.2), we arrive at *Gauss decomposition*

$$\mathbf{SL}(2,\mathbb{C}) \doteq \widetilde{\mathbf{N}}\mathbf{MAN} \tag{3.4}$$

where "$\doteq$" means that equality holds except a lower dimensional subset $p\mathbf{B}$ of the invariant measure 0. The map

$$\widetilde{\mathbf{N}} \times \mathbf{M} \times \mathbf{A} \times \mathbf{N} \to \mathbf{SL}(2,\mathbb{C}), \qquad (\widetilde{n}, m, a, n) \mapsto \widetilde{n}\,\mathrm{man}$$

is a diffeomorphism. If g decomposes under $\mathbf{SL}(2,\mathbb{C}) \doteq \widetilde{\mathbf{N}}\mathbf{MAN}$, we write $g \doteq \widetilde{n}(g)m(g)a(g)n$.

3.3 The Modular Function on the Borel Subgroup

Every Lie group $\mathbf{G}$ carries both left and right invariant measures: $d_l(hg) = d_l(g)$ and $d_r(gh) = d_r(g)$ for all $h \in \mathbf{G}$. Since they vanish on the same null sets, there is a measurable function, called the modular function, $\Delta_{\mathbf{G}} : \mathbf{G} \to \mathbb{R}_+$ such that $d_r g = \Delta_{\mathbf{G}}(g) d_l g$. If $\Delta_{\mathbf{G}} = 1$, the group is unimodular. The group $\mathbf{SL}(2,\mathbb{C})$ is unimodular and its invariant measure can be expressed as follows: If $g = \left(\begin{smallmatrix}\alpha & \beta\\ \gamma & \delta\end{smallmatrix}\right) \in \mathbf{SL}(2,\mathbb{C})$, then $dg = (1/|\delta|^2)\, d\beta\, d\overline{\beta}\, d\gamma\, d\overline{\gamma}\, d\delta\, d\overline{\delta}$, where, if $\beta = x + iy$, then $(i/2)\, d\beta\, d\overline{\beta} = dx\, dy$. This is not defined on the set of measure zero where $\delta = 0$. The Borel subgroup $\mathbf{B} \subset \mathbf{SL}(2,\mathbb{C})$ is not unimodular: If $b = \left(\begin{smallmatrix}\alpha & \beta\\ 0 & \alpha^{-1}\end{smallmatrix}\right) \in \mathbf{B}$, $d_l b = (i/2)^2(1/|\alpha|^4)\, d\alpha\, d\overline{\alpha}\, d\beta\, d\overline{\beta}$ and $d_r b = |\alpha|^4 d_l b$. Thus, the modular function on $\mathbf{B}$ is $\Delta_{\mathbf{B}}\left(\left(\begin{smallmatrix}\alpha & \beta\\ 0 & \alpha^{-1}\end{smallmatrix}\right)\right) = |\alpha|^4$.

4. The Principal Series Representations of $\mathbf{SL}(2,\mathbb{C})$

4.1 Induced Representations

To describe the method of inducing representations, we let $\mathbf{K}$ be a closed subgroup of a Lie group $\mathbf{G}$, both assumed unimodular with the invariant measures dk and dg, respectively.

Also, we assume that $\mathbf{G} = \mathbf{KP}$ with a closed subgroup $\mathbf{P}$, such that the map $(k,\ p) \mapsto kp$ of $\mathbf{K} \times \mathbf{P} \to \mathbf{G}$ is a bijection. Then the homogeneous (right coset) space $\mathbf{G}/\mathbf{P}$ is diffeomorphic to $\mathbf{K}$ on which $\mathbf{G}$ operates on the left.

Further, we let Π be a representation of $\mathbf{P}$ on a Hilbert space V and V^{Π} be the space of continuous mappings $f : \mathbf{G} \to V$ satisfying the condition

$$f(gp) = \Delta_{\mathbf{P}}(p)^{-1/2}\Pi(p)^{-1} f(g), \quad g \in \mathbf{G}, p \in \mathbf{P} \tag{4.1}$$

where $\Delta_{\mathbf{P}}$ is the modular function on $\mathbf{P}$. It shows that f is determined by its restriction to $\mathbf{K}$ and we can define the norm of f by

$$||f||^2 = \int_{\mathbf{K}} |f(k)|^2\, dk\ . \tag{4.2}$$

Finally, the representation $\mathcal{U}^{\Pi}$ of $\mathbf{G}$ on V^{Π} is given by the left regular action $\mathcal{U}^{\Pi}(g)$ $f(x) = f(g^{-1}x)$. The actual representation $\mathcal{U}^{\Pi}$ and the Hilbert space is obtained by completion in the L^2-norm in (4.2). $\mathcal{U}^{\Pi}$ is called the *induced representation* of Π to $\mathbf{G}$. The factor $\Delta_{\mathbf{P}}(p)^{-1/2}$ in (4.1) unitarizes the induces representation. In fact, one has the following result [17].

Proposition 1. *If the representation* Π *is unitary, then the induced representation* $\mathcal{U}^{\Pi}$ *is unitary.*

4.2 Inducing Representations of $\mathbf{SL}(2, \mathbb{C})$

In this section we apply the method of induction outlined in the previous section to obtain unitary representations of the group $\mathbf{SL}(2, \mathbb{C})$, referred to as the *principal series* of $\mathbf{SL}(2, \mathbb{C})$. We start with the following fact about the Borel subgroup $\mathbf{B} = \mathbf{MAN}$: Every finite-dimensional unitary irreducible representation of $\mathbf{B}$ is of the form [21]

$$\Pi(\text{man}) = \Pi_l(m)\Pi_s(a) = \left(\frac{\alpha}{|\alpha|}\right)^l |\alpha|^{is}, \quad l \in \mathbb{Z}, \quad s \in \mathbb{R}\ , \tag{4.3}$$

where man is given in (3.3). These one-dimensional representations are the characters of the Borel subgroup.

Next, following the general method of the previous section, we defined the action

$$\mathcal{T}^{\Pi}(g) f(x) = f\big(g^{-1}x\big) \tag{4.4}$$

on the space

$$V^{\Pi} = \Big\{ f \in C(\mathbf{SL}(2, \mathbb{C})) \mid f(g\,\text{man}) = \Pi(\text{man})^{-1}\Delta_{\mathbf{B}}(\text{man})^{-1/2} f(g) \Big\} \tag{4.5}$$

where $\Delta_{\mathbf{B}}(\text{man}) = |\alpha|^4$ is the modular function on $\mathbf{B} \subset \mathbf{SL}(2, \mathbb{C})$. Explicitly, any $f \in V^{\Pi}$ satisfies the conditions

$$f(g\,\text{man}) = |\alpha|^{-is-2}\left(\frac{\alpha}{|\alpha|}\right)^{-l} f(g), \quad l \in \mathbb{Z}, \quad s \in \mathbb{R}\ . \tag{4.6}$$

Further, Iwasawa decomposition shows that any $f \in V^{\Pi}$ is determined by the restriction $f\ |_{\mathbf{SU}(2)}$ and that the actual Hilbert space and unitary representations are obtained by completion in the norm (4.2) with $\mathbf{K} = \mathbf{SU}(2)$. In this realization of unitary representations, the action (4.4) is simple but the representation space (4.5) is complicated.

4.3 Noncompact Picture of Induced Representation

The noncompact picture is the realization of induced representations obtained by restricting functions in (4.5) to the subgroup $\widetilde{\mathbf{N}}$. It will be used to construct the noncompact model of projective Fourier analysis particularly accessible to analytical and fast numerical methods. A dense subspace of the representation is

$$V^{\Pi} = \left\{ f \in C\left(\widetilde{\mathbf{N}}\right) \mid f\left(\overline{n}\,\mathrm{man}\right) = \Pi(\mathrm{man})^{-1} \Delta_{\mathbf{B}}(\mathrm{man})^{-1/2} f\left(\widetilde{n}\right) \right\} \tag{4.7}$$

and the restriction is one-to-one because, by Gauss decomposition, the set $\widetilde{\mathbf{N}}\mathbf{MAN}$ exhausts $\mathbf{SL}(2,\mathbb{C})$ except for a measure zero set. In this picture, $\mathbf{SL}(2,\mathbb{C})$ acts on V^{Π} as follows: If $g = \left(\begin{smallmatrix} \alpha & \beta \\ \gamma & \delta \end{smallmatrix}\right) \in \mathbf{SL}(2,\mathbb{C})$ then

$$\begin{aligned} \mathcal{T}^{\Pi}(g) f\left(\widetilde{n}\right) &= f\left(g^{-1}\widetilde{n}\right) \\ &= f\left(\widetilde{n}\left(g^{-1}\widetilde{n}\right) m\left(g^{-1}\widetilde{n}\right) a\left(g^{-1}\widetilde{n}\right) n\right) \\ &= |-\beta z+\delta|^{-is-2} \left(\frac{-\beta z+\delta}{|-\beta z+\delta|}\right)^{-l} f\left(\begin{pmatrix} 1 & 0 \\ \frac{\alpha z-\gamma}{-\beta z+\delta} & 1 \end{pmatrix}\right). \end{aligned} \tag{4.8}$$

The next proposition, the proof of which follows an important technique in representation theory of semisimple Lie groups explained in detail in [17] on p. 140–141, says that the norms of $L^2(\mathbf{SU}(2), dk)$ and $L^2(\widetilde{\mathbf{N}}, d\widetilde{n})$ are preserved in passing from the induced picture to the noncompact picture.

Proposition 2. *For any $f \in C(\mathbf{SU}(2))$ that is right invariant under $\mathbf{M}$, that is, for any $f \in C(\mathbf{SU}(2)/\mathbf{M})$, we have that*

$$\int_{\mathbf{SU}(2)} |f(k)|^2 \, dk = \int_{\widetilde{\mathbf{N}}} \left| f\left(\widetilde{n}\right) \right|^2 d\widetilde{n} \, .$$

4.4 Compact Picture of Induced Representations

The compact picture is obtained by restricting the induced picture to $\mathbf{SU}(2)$. More precisely, one starts with $f \in C(\mathbf{SU}(\mathbf{2})/\mathbf{M})$ and extends it to a function on $\mathbf{SU}(\mathbf{2})$ by $f(\kappa m) = \Pi(m)^{-1} f(\kappa)$. Here a dense subspace of the representation is

$$V^{\Pi} = \left\{ f \in C(\mathbf{SU}(\mathbf{2})) \mid f(km) = \Pi(m)^{-1} f(k) \right\} \tag{4.9}$$

with norm (4.2). The restriction is one-to-one since Iwasawa decomposition, $\mathbf{SL}(2,\mathbb{C}) = \mathbf{SU}(\mathbf{2})\mathbf{MAN}$, implies that $\mathbf{SL}(2,\mathbb{C})/\mathbf{B} = \mathbf{SU}(\mathbf{2})/\mathbf{M}$ as a homogeneous space of $\mathbf{SU}(\mathbf{2})$.

Now, if g decomposes under $\mathbf{SU}(\mathbf{2})\mathbf{MAN}$ as

$$g = \kappa(g)\mu(g)a'(g)n \, , \tag{4.10}$$

then $\kappa(g) \in \mathbf{SU}(\mathbf{2})/\mathbf{M} \cong S^2$. We have that $\kappa(g) = k(g)\mathbf{M} = g\mathbf{MAN}$ in $\mathbf{SL}(2,\mathbb{C})/\mathbf{B}$ where $k(g)$ is given by Iwasawa decomposition $g = k(g)a'(g)n$ in (3.1). Using (4.6) and (4.10)

in (4.4), we obtain

$$\begin{aligned}\mathcal{T}^{\Pi}(g)f(k) &= f\left(g^{-1}k\right)\\ &= \Pi_s\left(a'\left(g^{-1}k\right)\right)^{-1}\Delta_{\mathbf{B}}\left(\mu\left(g^{-1}k\right)a'\left(g^{-1}k\right)n\right)^{-1/2}\\ &\quad\times\Pi_l\left(\mu\left(g^{-1}k\right)\right)^{-1}f\left(\kappa\left(g^{-1}k\right)\right)\end{aligned}\tag{4.11}$$

where Π_l and Π_s are given for the corresponding subgroups as in (4.3). This picture seems to be to complicated to construct a feasible (in image processing) model of projective Fourier analysis. However, since the representation space does not depend on s, the compact picture is useful to study the reduction of $g \mapsto \mathcal{T}^{\Pi}(g)$ to the subgroup $\mathbf{SU}(2)$. We will use it to construct the compact model of projective Fourier analysis.

5. Projective Fourier Analysis

Projective Fourier analysis is developed in the framework of representation theory of semisimple Lie groups by constructing the two realizations, the noncompact and the compact models.

5.1 Noncompact Realization of the Projective Fourier Analysis

The condition (4.6) implies that f must be $\mathbf{N}$-invariant, and therefore, it can be written as a function on $\mathbb{C}^2\backslash\{0\}$ (denoted by F) as follows: $F\binom{z_1}{z_2} = F\left(\binom{z_1}{z_2}\ \binom{\beta}{\delta}\binom{1}{0}\right)$. In the group-theoretic formalism, the group $\mathbf{N}$ is the isotropy group of $\binom{1}{0} \in \mathbb{C}^2\backslash\{0\}$, implying that $\mathbb{C}^2\backslash\{0\}$ is isomorphic to the homogeneous space $\mathbf{SL}(2,\mathbb{C})/\mathbf{N}$.

We verify that $f \in V^{\Pi}$, if and only, if the corresponding F on $\mathbf{SL}(2,\mathbb{C})/\mathbf{N}$ satisfies

$$F\left(\begin{pmatrix}\lambda z_1\\ \lambda z_2\end{pmatrix}\right) = \lambda^m\overline{\lambda}^n F\left(\begin{pmatrix} z_1\\ z_2\end{pmatrix}\right) = |\lambda|^{is-2}\left(\frac{\lambda}{|\lambda|}\right)^k F\left(\begin{pmatrix} z_1\\ z_2\end{pmatrix}\right)$$

where $m = (1/2)(k+is) - 1$ and $m = (1/2)(-k+is) - 1$. Thus, we can write, $F\binom{z_1}{z_2} = |z_1|^{is-2}(z_1/|z_1|)^k\,\Phi(z_2/z_1)$ where $\Phi(z) = F\binom{1}{z}$. At this point we are dealing with homogeneous functions F on $\mathbb{C}^2\backslash\{0\}$, the space of functions on which the irreducible representations of $\mathbf{SL}(2,\mathbb{C})$ were originally constructed in [9]. Now the principal series in (4.8) takes on the form

$$\mathcal{T}^{\Pi}\Phi(z) = |-\beta z+\delta|^{-is-2}\left(\frac{-\beta z+\delta}{|-\beta z+\delta|}\right)^{-k}\Phi\left(\frac{\alpha z-\gamma}{-\beta z+\delta}\right),$$

which extends to the principal series representation of $\mathbf{SL}(2,\mathbb{C})$ on $L^2(\mathbb{C})$.

Projective Fourier transform.

For a given pattern's intensity function $f(z)$ we place it on the image plane $z_1 = 1$ of the conformal camera by writing $h\left(\binom{1}{z}\right) \equiv f(z)$, and extend continuously to a subset of $\mathbb{C}^2$ along the complex lines as follows: $h\left(\binom{\xi}{\xi z}\right) = |\xi|^{-1} f(\xi z)$. First we note that the action of

$\mathbf{SL}(2,\mathbb{C})$ on h given by $h\big(g^{-1}\binom{z_1}{z_2}\big)$ induces the projective transformation $f(g^{-1}\cdot z)$ of the pattern f [26]. Next, we define functions

$$F\left(\begin{pmatrix} z_1 \\ z_2 \end{pmatrix}\right) = \frac{i}{2}\int h\left(\begin{pmatrix} \mu z_1 \\ \mu z_2 \end{pmatrix}\right)|\mu|^{-is}\left(\frac{\mu}{|\mu|}\right)^{-k} d\mu\, d\overline{\mu}$$

and verify that F is in the representation space V^{Π}. We express this F in terms of pattern's intensity function f and denote by $\Phi(z;k,s)$ its restriction to the image plane. Then, changing variable $\xi = \mu z$ yields $\Phi(z;k,s) = |z|^{is-1}\,(z/|z|)^k\,\widehat{f}(s,k)$ where

$$\widehat{f}(s,k) = \frac{i}{2}\int f(\xi)|\xi|^{-is-1}\left(\frac{\xi}{|\xi|}\right)^{-k} d\xi\, d\overline{\xi} \tag{5.1}$$

is the *projective Fourier transform (PFT)* of the pattern f. In log-polar coordinates (u,θ) given by $\xi = e^{u+i\theta}$, $\widehat{f}(k,s)$ has the form of the standard Fourier integral. Inverting it (see [26]), we get the *inverse projective Fourier transform*

$$f(z) = \frac{1}{(2\pi)^2}\sum_{k=-\infty}^{\infty}\int \widehat{f}(s,k)|z|^{is-1}\left(\frac{z}{|z|}\right)^k ds\ . \tag{5.2}$$

Further, the usual Plancherel's theorem gives the following projective counterpart of it:

$$\frac{i}{2}\int |f(z)|^2\, dz\, d\overline{z} = \frac{1}{(2\pi)^2}\sum_{k=-\infty}^{\infty}\int \big|\widehat{f}(s,k)\big|^2\, ds\ .$$

We see that the inverse projective Fourier transform provides decomposition in terms of the characters $|z|^{is}\,(z/|z|)^l$ of the Borel subgroup $\mathbf{B}$ with the coefficients given by the projective Fourier transform. We note that the Gauss decomposition $\mathbf{SL}(2,\mathbb{C}) \doteq \widetilde{\mathbf{N}}\mathbf{B}$ implies that $\mathbf{B}$ exhaust the "projective" part of $\mathbf{SL}(2,\mathbb{C})$ as $\widetilde{\mathbf{N}} \cong \mathbb{C}$, represent translations in the image plane. It should be seen in the light of the fact that all nontrivial unitary representations of the group $\mathbf{SL}(2,\mathbb{C})$ are infinite-dimensional [9], as opposed to the fact we have mentioned before that all finite-dimensional irreducible unitary representations of the Borel group $\mathbf{B}$ are in fact one-dimensional.

The *convolution* in noncompact picture is defined on the subgroup $\mathbf{MA}$ by

$$f_1 * f_2(z) = \frac{i}{2}\int f_1(\xi)\, f_2\big(g^{-1}\cdot z\big)\frac{d\xi\, d\overline{\xi}}{|\xi|^2} \tag{5.3}$$

where $g = \left(\begin{smallmatrix}\delta^{-1/2} & 0\\ 0 & \delta^{1/2}\end{smallmatrix}\right)\left(\begin{smallmatrix}e^{-i\varphi/2} & 0\\ 0 & e^{i\varphi/2}\end{smallmatrix}\right)$ and $\xi = \delta e^{i\varphi}$. Then, taking the projective Fourier transform of the convolution (5.3) and changing the variable by $\eta = \xi^{-1}z$, we easily obtain the *convolution property*: $\widehat{f_1 * f_2}(k,s) = \widehat{f_1}(k,s)\,\widehat{f_2}(k,s)$.

5.2 Compact Realization of Projective Fourier Analysis

Recall that the compact realization is constructed by using the compact picture of induced representation with the action (4.11) reduced to the subgroup $\mathbf{SU}(2)$. This reduction problem can be formulated as follows (see also [1] for a more general discussion).

Proposition 3. *If $\mathcal{T}^{\Pi}$ is an irreducible representation of $\mathbf{SL}(2,\mathbb{C})$ induced from an irreducible representation Π of the Borel subgroup $\mathbf{B}$, and $\mathcal{R}$ is an irreducible representation of $\mathbf{SU}(2)$, then $\mathcal{R}$ is in $\mathcal{T}^{\Pi}_{\mathbf{SU}(2)}$ (the restriction of $\mathcal{T}^{\Pi}$ to $\mathbf{SU}(2)$) with multiplicity one.*

We recall that in the compact picture a dense subspace of the representation space is (4.9) with norm (4.2) and the action of induced unitary representations of $\mathbf{SL}(2,\mathbb{C})$ is given in (4.4). It reduces to the following action

$$\begin{aligned}\mathcal{T}^{\Pi_{l,s}}_{\mathbf{SU}(2)}(k)f(k_1) &= f\left(k^{-1}k_1\right)\\ &= \Pi_l\left(\mu\left(k^{-1}k_1\right)\right)^{-1} f\left(\kappa\left(k^{-1}k_1\right)\right), \quad f\in V^{\Pi}\,.\end{aligned}$$

Here for any $k\in\mathbf{SU}(2)$ we have the factorization $k=\kappa(k)\mu(k)$ where $\kappa(k)=k\mathbf{M}\in \mathbf{SU}(2)/\mathbf{M}$ and $\mu(k)\in\mathbf{M}$. It shows that $f\in V^{\Pi}$ is determined by $f\mid_{\mathbf{SU}(2)/\mathbf{M}}$ and that $||f(k\mathbf{M})||=||f(k)||$.

In the remaining part of this section, we discuss the relation between $\mathbf{SU}(2)/\mathbf{M}$ and $\mathbf{SO}(3)/\mathbf{SO}(2)$ in the context of the conformal camera and, then we construct the compact realization of projective Fourier analysis. Finally, we prove Proposition 3.

The relation between $\mathbf{SU}(2)/\mathbf{M}$ and $\mathbf{SO}(3)/\mathbf{SO}(2)$.

Using the universal double cover $\mathbf{SU}(2)$ of $\mathbf{SO}(3)$, used in Section 2.3 to get the conformal camera model shown in Figure 1, we have the diagram

$$\begin{array}{ccc}\mathbf{SU}(2) & \overset{\Phi}{\to} & \mathbf{SO}(3)\\ {\scriptstyle\pi_1}\downarrow & & \downarrow{\scriptstyle\pi_2}\\ P^1(\mathbb{C}) & \overset{\sigma}{\to} & \mathbf{S}^2_{(0,1,0)}\end{array} \tag{5.4}$$

where π_1 and π_2 are the projections onto the quotient spaces $\mathbf{SU}(2)/\mathbf{M}\cong P^1(\mathbb{C})$ and $\mathbf{SO}(3)/\mathbf{SO}(2)\cong\mathbf{S}^2_{(0,1,0)}$, respectively. The mapping $\sigma: P^1(\mathbb{C})\to\mathbf{S}^2_{(0,1,0)}$ is the inverse of the stereographic projection (2.3), given explicitly by

$$\sigma(z)=\left(\frac{2\,\mathrm{Im}\,z}{|z|^2+1},\frac{2}{|z|^2+1},\frac{2\,\mathrm{Re}\,z}{|z|^2+1}\right)^t=(y_1,y_2,y_3)^t$$

and $\sigma(\infty)=(0,0,0)^t$. We note that $(y_1)^2+(y_2-1)^2+(y_3)^2=1$.

By a straightforward calculation we can obtain the relation $\Phi(k)\circ\sigma=\sigma\circ k,\ \ k\in\mathbf{SU}(2)$. This can be verified by writing both sides in explicit terms. On one hand side, we have $\sigma\circ k(z)=\sigma\left(k(\psi,\phi,\psi')\cdot z\right)=(y_1',y_2',y_3')^t$ where $k(\psi,\phi,\psi')$ in (2.4) gives the linear fractional action:

$$k\left(\psi,\phi,\psi'\right)\cdot z=\frac{\cos\left(\frac{\phi}{2}\right)e^{-i(\psi+\psi')/2}z+i\sin\left(\frac{\phi}{2}\right)e^{-i(\psi-\psi')/2}}{i\sin\left(\frac{\phi}{2}\right)e^{i(\psi-\psi')/2}z+\cos\left(\frac{\phi}{2}\right)e^{i(\psi+\psi)/2}}\,.$$

On the other hand, side, $\Phi(k(\psi,\phi,\psi'))\circ\sigma(z)=(y_1',y_2',y_3')^t$ where $\Phi(k(\psi,\phi,\psi'))=R(\psi,\phi,\psi')$ acts on $\mathbf{S}^2_{(0,1,0)}$ i.e.,

$$\Phi\left(k\left(\psi,\phi,\psi'\right)\right)\circ\sigma(z)=R\left(\psi,\phi,\psi'\right)\left[\sigma(z)-(0,1,0)^t\right]+(0,1,0)^t\,.$$

Thus, $(y_1')^2+(y_2'-1)^2+(y_3')^2=1$.

In conclusion, the diagram (5.4), represent a homomorphism of homogeneous spaces, $P^1(\mathbb{C})\cong\mathbf{SU}(2)/\mathbf{M}$ and $\mathbf{S}^2_{(0,1,0)}\cong\mathbf{SO}(3)/\mathbf{SO}(2)$.

Projective Fourier transform.

It follows from the homomorphisms Φ and σ in (5.4), and the spherical harmonic analysis [6], that the regular representation of the group $\mathbf{SU}(2)$ on $L^2(\mathbf{SU}(2)/\mathbf{M}, dk)$ where dk is the $\mathbf{SU}(2)$-invariant measure on $\mathbf{SU}(2)/\mathbf{M}$, is a direct sum of representations $\mathcal{D}^{(l)} \circ \Phi$; $l \in \mathbb{N}$ where $\mathcal{D}^{(l)}$ (corresponding to $D^{(l)}$ in [6]) are irreducible unitary representations of $\mathbf{SO}(3)$, with each $\mathcal{D}^{(l)} \circ \Phi$ occurring only once in this sum. The standard fact is that the representation $\mathcal{R}^{(l)}$ of $\mathbf{SU}(2)$ defines a representation $\mathcal{D}^{(l)}$ of $\mathbf{SO}(3)$ by means of formula $\mathcal{D}^{(l)} \circ \Phi = \mathcal{R}^{(l)}$, if and only, if l is an integer. Thus, the harmonic decompositions of functions on $P^1(\mathbb{C}) \cong \mathbf{SU}(2)/\mathbf{M}$ should be given with respect to the *projective harmonics* $Y_l^m \circ \sigma$ on $P^1(\mathbb{C})$, where Y_l^m are spherical harmonics given in Equation (1) in [6].

To this end, we note that the subgroup $\mathbf{M}$ of elements $m\left(\frac{\psi}{2}\right) = \left(\begin{smallmatrix} e^{-i\psi/2} & 0 \\ 0 & e^{i\psi/2} \end{smallmatrix}\right)$ is the isotropy group at $0 \in \mathbb{C}$ and its action on the image plane $\mathbb{C}$ (an open affine patch of $\widehat{\mathbb{C}}$) consists of rotations of angle ψ about the origin. Further, the subgroup $\mathbf{K}$ of elements $k\left(\frac{\phi}{2}\right) = \left(\begin{smallmatrix} \cos\phi/2 & i\sin\phi/2 \\ i\sin\phi/2 & \cos\phi/2 \end{smallmatrix}\right)$ moves the point 0 of $\mathbb{C}$ along the positive imaginary axis for $0 \le \phi < \pi$. Thus, we have the parametrization of the image plane by the polar coordinates, $z = \tan\frac{\phi}{2} e^{i\psi}$, expressed in terms of the Euler angles.

Using this, we can find the relation between the rotational-invariant measures $d\omega$ on $\mathbf{S}^2_{(0,1,0)}$ and the $\mathbf{SU}(2)$-invariant measure $d\varrho$ on $\mathbb{C}$. Indeed, for the measure $d\omega = \sin\phi\, d\phi\, d\psi$ on $\mathbf{S}^2_{(0,1,0)}$, its pullback $\sigma^*(d\omega)$ by the mapping $\sigma : \mathbb{C} \to \mathbf{S}^2_{(0,1,0)}$ is a measure on $\mathbb{C}$. A straightforward calculation, using the relation $z = \tan\frac{\phi}{2} e^{i\psi}$, gives $d\varrho(z) = \sigma^*(d\omega) = 2i\left(1+|z|^2\right)^{-2} dz\, d\overline{z}$, which has the desired invariance property, $d\varrho(g^{-1}\cdot z) = d\varrho(z)$, $g \in \mathbf{SU}(2)$.

The projective harmonics, $Z_l^m(z) = Y_l^m \circ \sigma(z)$, are now expressed on $\mathbb{C}$ as follows:

$$Y_l^m \circ \sigma\left(re^{i\varphi}\right) = (-1)^m \sqrt{\frac{(2l+1)(l-m)!}{4\pi(l+m)!}} P_l^m\left(\frac{1-r^2}{1+r^2}\right) e^{im\varphi}, \quad z = re^{i\varphi}$$

where $l \in \mathbb{N}$, $-l \le m \le l$. Choosing the basis of $2l+1$ spherical harmonics Y_l^m, $-l \le m \le l$ for each $l \ge 0$ gives an orthonormal basis $Z_l^m(z)$; $-l \le m \le l$, for all of $L^2(\mathbb{C}, d\varrho)$.

Now, by analogy with the harmonic analysis in $L^2(\mathbf{SO}(3)/\mathbf{SO}(2), d\omega)$, we obtain the decomposition of $f \in L^2(\mathbb{C}, d\varrho)$ in the orthonormal basis provided by the projective harmonics in the form

$$f(z) = \sum_{l\in\mathbb{N}} \sum_{|m|\le l} \widehat{f}(l,m) Z_l^m(z) \tag{5.5}$$

where the coefficients $\widehat{f}(l,m)$ of the decomposition are given by the Fourier transform

$$\widehat{f}(l,m) = \int_{\mathbb{C}} f(z)\overline{Z}_l^m(z) 2i \left(1+|z|^2\right)^{-2} dz\, d\overline{z}\,. \tag{5.6}$$

We call (5.6) the *projective Fourier transform in compact picture.* Its inverse transform is given in (5.5). Using the following notation: $\mathcal{R}^{(l)} = \left(R^{(l)}_{m,k}\right)$, $\mathcal{D}^{(l)} = \left(D^{(l)}_{m,k}\right)$, $R^{(l)}_{m,k} = D^{(l)}_{m,k} \circ \Phi$ and $\omega = \sigma(z)$, and the fact that the representation $\mathcal{D}^{(l)}$ is unitary, that is, $\overline{D}^{(l)}_{k,m}(R) = D^{(l)}_{m,k}(R^{-1})$, the projectively covariant characteristics of the harmonic decomposition of the function $f(z)$ in the basis $Z_l^m(z)$ is demonstrated in the next theorem,

which can be proved along similar lines of the corresponding proof given for spherical harmonic analysis in [6].

Theorem 1. *The decomposition*

$$f(z) = \sum_{l\in\mathbb{N}} \sum_{|m|\le l} \widehat{f}(l,m) Z_l^m(z)$$

under the projective transformation $\mathcal{R}(g)\ f(z) = f(g^{-1}\cdot z)$ *transforms as follows*

$$\mathcal{R}(g) f(z) = \sum_{l\in\mathbb{N}} \sum_{|k|\le l} \left(\sum_{|m|\le l} \widehat{f}(l,m) \overline{R}^{(l)}_{m,k}\big(g^{-1}\big) \right) Z_l^k(z)$$

where for each $l \in \mathbb{N}$

$$\mathcal{R}^{(l)}(g) = \mathcal{D}^{(l)} \circ \Phi(g) \tag{5.7}$$

with $\mathcal{D}^{(l)}$ (*corresponding to* $D^{(l)}$ *in [6]*) *and* Φ *in* (5.4)*, is the irreducible unitary representation of* $\mathbf{SU}(2)$ *on the Hilbert space* $W^l = \left\{ Z_l^m(z) : l \in \mathbb{N}, -l \le m \le l \right\}$ *with the inner product*

$$\langle f, h\rangle = \int f(z)\overline{h}(z) 2i \left(1 + |z|^2\right)^{-2} dz\, d\overline{z}\ .$$

The Plancherel formula here takes on the following form:

$$||f||^2_{L^2(\mathbb{C},d\varrho)} = \sum_{l=0}^{\infty} \sum_{|m|\le l} \left|\widehat{f}(l,m)\right|^2\ ,$$

which says that the mapping $f(z) \longmapsto \widehat{f}(l,m)$ is isometric with respect to the corresponding norms.

For two functions f_1 and f_2 on $\mathbb{C}$ the operator of left convolution *by* f_1 is defined by

$$\begin{aligned} \mathfrak{C}_{f_1} f_2(z) &= \int_{\mathbf{SU}(2)} f_1(g\cdot 0)\mathcal{R}(g) f_2(z)\, dg \\ &= \int_{\mathbf{SU}(2)} f_1(g\cdot 0) f_2\big(g^{-1}\cdot z\big)\, dg = f_1 * f_2(z)\ . \end{aligned} \tag{5.8}$$

Since the operators $\mathcal{R}(g)$ are simultaneously block-diagonalized for all $g \in \mathbf{SU}(2)$ in the projective harmonic basis Z_l^m (because $\mathcal{D}^{(l)}$ are simultaneously block-diagonalized in the basis Y_l^m), therefore the convolution operator $\mathfrak{C}_{f_1}$ obtained as linear combination of them must be block-diagonalized as well. An explicit statement of this is given in the next theorem. A proof involves the relation between $\mathcal{R}^{(l)}(g)$, $\mathcal{D}^{(l)}(g)$ and Φ stated before Theorem 1 and otherwise can be done along the same lines as the corresponding proof for spherical Fourier analysis in [6].

Theorem 2. *The convolution property*

$$\widehat{f_1 * f_2}(l,m) = 2\pi \left(\frac{4\pi}{2l+1}\right)^{1/2} \widehat{f}_1(l,m)\, \widehat{f}_2(l,m) \tag{5.9}$$

is satisfied.

The reduction problem for the compact picture.

To prove Proposition 3, we use the compact picture of induced representations of $\mathbf{SL}(2,\mathbb{C})$. To this end, we let

$$\Pi_{k,s}(b) = \Pi_k\left(\mu(b)\right)\Pi_s\left(a'(b)\right) = e^{ik\varphi}|\rho|^{is}, \quad b = \begin{pmatrix} \rho e^{i\varphi} & \beta \\ 0 & \rho^{-1}e^{-i\varphi} \end{pmatrix} \in \mathbf{B}$$

be the unitary representation of $\mathbf{B} = \mathbf{MAN}$. An irreducible representation $\mathcal{R}^{(l)}$ of $\mathbf{SU}(2)$, determined by l where $2l = 0, 1, 2, \ldots$, is expressed with respect to the basis of the projective harmonics Z_l^n, $n = -l, -l+1, \ldots, l-1, l$. In the Euler angle parametrization introduced in Section 2.3, $m(\psi/2) \in \mathbf{M}$ corresponds to the rotation around x_2-axis by the angle ψ. Hence, $\mathcal{R}^{(l)}(m(\psi/2))\, Z_l^n = \exp(-in\psi) Z_l^n$, and every representation $\psi \mapsto \exp(-in\psi)$ of $\mathbf{M}$ appears with multiplicity one. Consequently, $\mathcal{R}^{(l)}$ reduced to $\mathbf{M}$, that is, $\mathcal{R}^{(l)}_{\mathbf{M}}$ contains $(\Pi_{\mathbf{M}})_{k,s} = \Pi_k$, if and only, if k is one of the numbers $l, l-1, \ldots, -l$. Thus, $l \geq k$, the representation $\mathcal{R}^{(l)}$ enters $\mathcal{T}^{\Pi}_{\mathbf{SU}(2)}$ with the multiplicity one, i.e.,

$$\mathcal{T}^{\Pi}_{\mathbf{SU}(2)} = \bigoplus_{l \geq |k|} \mathcal{R}^{(l)}\left(\mathbf{SU}(2)\right) \ .$$

It proves Proposition 3.

6. Applications in Computational Vision

In this section we discuss analytical aspects of the data model of the digital image representation based on the noncompact projective Fourier transform and some of its applications in computational vision, both in biology and computer science. We also mention the uses of projective convolutions to perform tasks of perspectively-invariant pattern matching. We start with the derivation of the discrete projective Fourier transform.

6.1 The Discrete Projective Fourier Transform

In log-polar coordinates (u, θ) given by $z = e^u e^{i\theta}$, (5.1) has the standard Fourier integral form

$$\widehat{f}(s,k) = \int_0^{2\pi/L} \int_{\ln r_a}^{\ln r_b} g(u,\theta) e^{-i(us+\theta k)}\, du\, d\theta \tag{6.1}$$

where the support of $g(u,\theta) = e^u f(e^{u+i\theta})$ is assumed to be contained within $[\ln r_a, \ln r_b] \times [0, 2\pi/L]$ with $L \in \mathbb{N}$. Extending $g(u,\theta)$ periodically $g(u+mT, \theta + 2\pi n/L) = g(u,\theta)$, where $T = \ln \frac{r_b}{r_a}$, it can be expanded in a double Fourier series (see [27]):

$$g(u,\theta) = \frac{L}{2\pi T} \sum_{m=-\infty}^{\infty} \sum_{n=-\infty}^{\infty} \widehat{f}\,(2\pi m/T, nL)\, e^{i(2\pi mu/T + nL\theta)} \ .$$

Further, assuming

$$\operatorname{supp} \widetilde{g} = \operatorname{supp} \widehat{f} \subset [-\Omega, \Omega] \times [-\Gamma, \Gamma] \tag{6.2}$$

($\widetilde{g}$ is the Fourier transform of g) and approximating the integral in (6.1) by a double Riemann sum with $M \times N$ partition points $(u_k, \theta_l) = (\ln r_a + kT/M, 2\pi l/LN)$; $0 \le k \le M-1$, $0 \le l \le N-1$, we obtain

$$\widehat{f}\,(2\pi m/T, nL) \approx \frac{2\pi T}{LNM} \sum_{k=0}^{M-1} \sum_{l=0}^{N-1} g(u_k, \theta_l) e^{-2\pi i (mk/M + nl/N)}$$

where $|m| \le \Omega T/2\pi$ and $|n| \le \Gamma/L$. Following the discussion of the numerical aspects of the approximation in [13], we obtain the expressions

$$\widehat{f}_{m,n} = \sum_{k=0}^{M-1} \sum_{l=0}^{N-1} \mathrm{f}_{k,l}\, e^{u_k} e^{-i2\pi nl/N} e^{-i2\pi mk/M} \tag{6.3}$$

and

$$\mathrm{f}_{k,l} = \frac{1}{MN} \sum_{m=0}^{M-1} \sum_{n=0}^{N-1} \widehat{f}_{m,n} e^{-u_k} e^{i2\pi nl/N} e^{i2\pi mk/M} \tag{6.4}$$

where $\mathrm{f}_{k,l} = (2\pi T/LMN) g(u_k, \theta_l) e^{-u_k}$ and $\widehat{f}_{m,n} = \widehat{f}\,(2\pi m/T, nL)$. Both expressions (6.3) and (6.4) can be computed efficiently by FFT algorithms.

Finally, on introducing $z_{k,l} = e^{u_k + i\theta_l}$ into (6.3) and (6.4) we arrive at the (M, N)-*point discrete projective Fourier transform (DPFT)* and its *inverse*:

$$\widehat{f}_{m,n} = \sum_{k=0}^{M-1} \sum_{l=0}^{N-1} f_{k,l} \left(\frac{z_{k,l}}{|z_{k,l}|} \right)^{-nL} |z_{k,l}|^{-i2\pi m/T + 1} \tag{6.5}$$

and

$$f_{k,l} = \frac{1}{MN} \sum_{m=0}^{M-1} \sum_{n=0}^{N-1} \widehat{f}_{m,n} \left(\frac{z_{k,l}}{|z_{k,l}|} \right)^{nL} |z_{k,l}|^{i2\pi m/T - 1}\,, \tag{6.6}$$

now with $f_{k,l} = (2\pi T/LMN) f(z_{k,l})$. Its *projectively adapted characteristics* are expressed as follows:

$$f'_{k,l} = \frac{1}{MN} \sum_{m=0}^{M-1} \sum_{n=0}^{N-1} \widehat{f}_{m,n} \left(\frac{z'_{k,l}}{|z'_{k,l}|} \right)^{nL} |z'_{k,l}|^{i2\pi m/T - 1} \tag{6.7}$$

where $z'_{k,l} = g^{-1} \cdot z_{k,l}$, $g \in \mathbf{SL}(2, \mathbb{C})$ and $f'_{k,l} = (2\pi T/LMN) f(z'_{k,l})$.

6.2 DPFT in Digital Image Processing

DPFT has the standard Fourier integral form in the log-polar coordinate plane. Therefore, in order to convert an analog image to the digital form and to display it in the image (viewing) plane by computing its DPFT with FFT, we must re-sample the image so that the sampling geometry in the log-polar coordinate plane consists equal rectangular samples (pixels). We refer to it as the sampling interface.

With the pattern domain contained within the set $[r_a, r_b] \times [0, 2\pi/L]$, the samples of the log-polar sampling are obtained by taking the radial and angular partitions,

$$r_k = r_a e^{k\delta_1}, \quad k = 0, 1, \ldots, M; \qquad \alpha_l = l\delta_2, \quad l = 0, 1, \ldots, N\ , \tag{6.8}$$

respectively. Thus, the pixels are sectors that have fixed angular size with their radial size increased logarithmically, see Figure 3 (A).

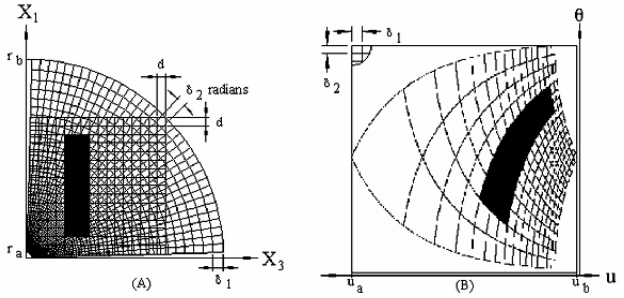

FIGURE 3 The sampling interface: (A) nonuniformly sampled retinal image, (B) uniformly sampled cortical image.

The minimal rate of the log-polar sampling depends on the resolution of the image. We require for our calculations that the upper right pixel is covered by one sector of the log-polar partition whose area is approximately the area of the pixel, see Figure 3 (A). The log-polar sampling geometry becomes again uniform with rectangular pixels $\delta_1 \times \delta_2$, shown for clarity only in the left corner of Figure 3 (B). To determine δ_1 and δ_2, or equivalently the resolution $M \times N$, we assume that the pattern size in the image plane is $A \times A$ and the pixels size is $d \times d$. Then, a simple geometrical consideration using the radial partition in (6.8) gives (see Figure 3) the following relations between dimensions of pixels: $\delta_1 = -\ln(1 - d/r_b) = (d/r_b) - (d/r_b)^2 + \ldots$, and $\delta_2 = d/r_b$ radians, where $r_b = r_a + \sqrt{2}A$. Because in practice $d \ll r_b$, we can take $\delta_1 = \delta_2 = \delta$ where $\delta = d/r_b$. Now, using (6.8), the resolution $M \times N$ of the image in log-polar coordinates is given by $M = (r_b/d)\ln(r_b/r_a)$ and $N = \pi r_b/(2d)$. For the bar pattern shown in Figure 3 (A) we take $L = 4$, $A = 16$, $r_a = 0.5$ and $d = 1$ (in units of pixels) and we obtain: $\delta = 0.04$, $M = 89$ and $N = 35$. However, the bar pattern in Figure 3 (B) has been rendered in the log-polar coordinate plane, using the sampling interface algorithm, with an increased resolution of 300×300 to smoothen pixel boundaries.

Band-limited images.

Often one can assume that a given pattern has a bounded spectrum, say $[-\omega, \omega] \times [-\omega, \omega]$. The value of ω could be determined, for example, by the rate at which the (standard) Fourier transform of the pattern is decaying for large spatial frequencies. The *Nyquist condition* requires that the sampling distance d satisfies the relation $d = \pi/\omega$ in both the x- and y-axis directions. Recalling that in the log-polar plane $\delta = T/M = 2\pi/LN$, we have $M = \omega r_b T/\pi$ and $N = 2\omega r_b/L$, where $T = \ln \frac{r_b}{r_a}$. We can obtain the log-polar radial and angular frequencies Ω and Γ [cf. (6.2)] corresponding to the spatial frequency ω by assuming the Nyquist condition: $\delta = \pi/\Omega = \pi/\Gamma$. We conclude that $\Omega = \Gamma = (r_a + \sqrt{2}A)\omega$.

Rendering digital image perspective transformations.

In this section we test the perspective covariance of the digital data model. However, in applications one can work equally well with image projective transformations without removing their conformal components. To simplify the discussion, we consider the subgroup of image projective transformations of the form

$$z'_{m,n} = g^{-1} \cdot z_{m,n} = \frac{z_{m,n}\cos\frac{\phi}{2} - i\sin\frac{\phi}{2}}{-iz_{m,n}\sin\frac{\phi}{2} + \cos\frac{\phi}{2}} \,. \tag{6.9}$$

Under the transformations (6.9), the equally spaced points (u_m, θ_n) transform into nonuniformly spaced points $(u'_{m,n}, \theta'_{m,n})$ with the coordinates satisfying the equations

$$e^{2u'_{m,n}} = \frac{e^{2u_m}\cos^2\frac{\phi}{2} + \sin^2\frac{\phi}{2} - e^{u_m}\sin\phi\sin\theta_n}{e^{2u_m}\sin^2\frac{\phi}{2} + \cos^2\frac{\phi}{2} + e^{u_m}\sin\phi\sin\theta_n} \tag{6.10}$$

and

$$\tan\theta'_{m,n} = \frac{1/2\big(e^{2u_m}-1\big)\sin\phi + e^{u_m}\sin\theta_n\cos\phi}{e^{u_m}\cos\theta_n} \,. \tag{6.11}$$

Finally, the coordinates (2.8) of the projectively transformed pixels can be used in a straightforward way to correct for conformal distortions of log-polar coordinates $(u'_{m,n}, \theta'_{m,n})$ given in (6.10) and (6.11). Those corrected log-polar coordinates are denoted by $(u''_{m,n}, \theta''_{m,n})$, in terms of which the *conformal-distortion free inverse DPFT* is given as follows

$$\mathrm{f}''_{m,n} = \frac{1}{MN}\sum_{k=0}^{M-1}\sum_{l=0}^{N-1} \widehat{f}_{k,l}\, e^{-u''_{m,n}} e^{i2\pi u''_{m,n}k/T} e^{i\theta''_{m,n}lL} \,. \tag{6.12}$$

Here $\mathrm{f}''_{m,n}$ denotes the value $f''_{m,n}$ given in (6.7) but taken at $(u''_{m,n}, \theta''_{m,n})$ such that

$$z''_{m,n} = x''_{3m.n} + ix''_{1m.n} = e^{u''_{m,n}} e^{i\theta''_{m,n}}$$

where $x''_{3m.n}$ and $x''_{1m.n}$ are given in (2.8).

Our tests of the perspective covariance are done by applying image projective transformations to the pixel's boundaries. In Figure 4, the deconformalized image projective transformations of the bar pattern in Figure 3 (A) are displayed in the log-polar coordinate plane for the two indicated values of ϕ in (6.9).

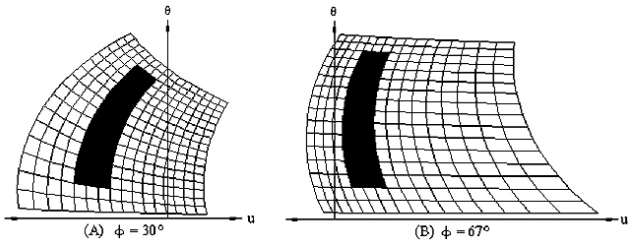

FIGURE 4 Deconformalized image projective transformations of the bar pattern in the log-polar plane.

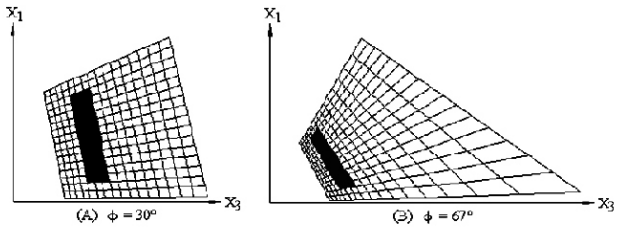

FIGURE 5 Image perspective transformations rendered in the image plane by using the sampling interface.

Next the outputs from the sampling interface algorithm, applied to the images in Figure 4 are shown in Figure 5. We see in this figure the corresponding image perspective (deconformalized image projective) transformations of the bar in the image plane.

The recent advances in nonuniform FFT (e.g., [7, 20]) allow the development of efficient algorithms reconstructing $f''_{m,n}$ from known $\widehat{f}_{k,l}$ by computing (6.12). However, (6.12) gives image perspective transformations in the log-polar coordinate plane. Therefore, to render them in the viewing image plane, the algorithm of the sampling interface transforming the corresponding sampling geometries must be used again.

DPFT and biologically motivated machine vision.

This section should be read together with Section 2.4 where the relation between the conformal camera and the computational visual neuroscience has been emphasized. The resampling from the image plane to the log-polar coordinate plane, referred to as the sampling interface, provides a well-known example of the foveated—as it provides the mathematical model of biological retina sensors—image representation used in certain computer vision systems, see for example, [2, 22]. The data processing reduction and similarity invariance advantages, of the log-polar sampling (Section 2.4) motivated the development of foveated sensor architectures, called silicon retina, in machine vision systems consisting of moving stereo camera head coupled with a hardware image processor and linked to the computer performing the image analysis. However, due to the lack of image processing tools that are explicitly designed for foveated vision, silicon retina sensors have not been widely used in the machine vision systems [31]. Because the image processing based on DPFT naturally involves the log-polar sampling, it is well adapted to both the retinotopic-like mapping of the silicon retina image processor and the image perspective transformations of patterns. We believe that it should provide the image processing tools needed for the biologically motivated machine vision systems.

Perspectively-invariant pattern matching.

The discrete convolution in the noncompact model of projective Fourier analysis can be computed efficiently by FFT. On the other hand, in the compact model of projective Fourier analysis, the projective Fourier transform and convolutions could be computed by adapting some of fast algorithms recently developed for spherical Fourier analysis. In analogy with the problem of pattern matching in Euclidean geometry, by taking the convolution in the compact model of projective Fourier analysis (the projective convolution over the double cover of the group of 3-D rotations) of a photograph and a pattern, we can locate the pattern in the photograph independent of its different perspective under rotations. Similarly, using the convolution in the noncompact model of projective Fourier analysis, allows development of an algorithm for pattern matching independent of similarity transformations.

7. Conclusions

In this article, projective Fourier analysis—geometric Fourier analysis of the group $\mathbf{SL}(2, \mathbb{C})$ that provides image projective transformations—is presented in the framework of representation theory of semisimple Lie groups. It consists of the two models, the noncompact and the compact models of projective Fourier analysis, constructed in the noncompact and the (reduced) compact pictures of induced unitary irreducible representations of $\mathbf{SL}(2, \mathbb{C})$, respectively. The data model for digital image representation is developed and its analytical properties are discussed in the framework of the noncompact discrete projective Fourier transform (DPFT). This discrete projective Fourier transform has the form of the standard Fourier integral in log-polar coordinates. Therefore, to convert analog images to the digital form and compute their DPFT by FFT, the image must be re-sampled on the log-polar grid. This log-polar geometry of sampling provides a foveated image representation that models the retinotopic mapping of the brain's visual pathway. Therefore, it supplies computational framework to develop efficient algorithms for biologically motivated machine vision systems. The data model is also well adapted to the image transformations produced by the changes in the perspective view of the same planar object, or pattern.

In conclusion, the digital data model of image representation developed in this article is well suited to provide the image processing tools explicitly designed for the foveated sensor architecture (silicon retina) of active vision systems. In particular, convolutions properties in both models of projective Fourier analysis can be used to develop perspectively-independent pattern matching algorithms. We note that due to the lack of elegant image processing tools for foveated vision, silicon retina sensors have not been widely used in machine vision systems.

References

[1] Barut, A. O. and Raczka, R. (1977). Theory of group representations and applications, PWN-Polish Scientific Publishers, Warszawa.

[2] Bederson, E. B., Wallece, R. S., and Schwartz, E. (1995). A miniaturized space-variant active vision systems: Cortex-1, *Machine Vision and Applications* **8**, 101–109.

[3] Berger, M. (1987). *Geometry I,* Springer-Verlag, New York.

[4] Brannan, D. A., Esplen, M. F., and Gray, J. J. (1998). *Geometry,* Cambridge University Press, Cambridge.

[5] Choquet-Bruhat, Y. and DeWitt-Morette, C. (1977). *Analysis, Manifolds and Physics,* 2nd ed., North-Holland, New York.

[6] Driscoll, J. R. and Healy, D. M. (1994). Computing Fourier transforms and convolutions on the 2-sphere, *Adv. in Appl. Math.* **15**, 202–250.

[7] Duijndam, A. J. W. and Schonewille, M. A. (1999). Nonuniform fast Fourier transform, *Geophysics* **64**, 539–551.

[8] Feichtinger H. G. and Strohmer, T., Eds., (1998). *Gabor Analysis and Algorithms. Theory and Applications,* Birkhäuser, Boston.

[9] Gelfand, I. M., Graev, M. I., and Vilenkin, N. Ya. (1966). *Generalized Functions Vol. 5: Integral Geometry and Representation Theory,* Academic Press, New York.

[10] Gonzales, R. C. and Wintz, P. (1987). *Digital Image Processing,* 2nd ed., Addison-Wesley Publ. Comp., Reading, MA.

[11] Helgason, S. (1993). The Fourier transforms on symmetric spaces and applications, in *Differential Geometry and Its Applications, Proceedings of the 5th International Conference,* 23–28, Kowalski, O. and Krupka, D., Eds., held in Opava, Czechoslavakia, August 24-28, (1992).

[12] Henle, M. (1997). *Modern Geometries. The Analytical Approach,* Prentice-Hall, Upper Saddle River, NJ.

[13] Henrici, P. (1986). *Applied and Computational Complex Analysis,* Vol. 3., John Wiley & Sons, New York.

[14] Herb, R. A. (2000). An elementary introduction to Harish-Chandra's work, in *The Mathematical Legacy of Harish-Chandra—A Celebration of Representation Theory and Harmonic Analysis,* Doran, R. S. and Varadarajan, V. S., Eds., *AMS Proceedings on Symposia in Pure Mathematics* **68**, 59–75.

[15] Hubel, D. E. (1988) *Eye, Brain, and Vision,* New York Scientific American Library.

[16] Jones, G. and Singerman, D. (1987). *Complex Functions,* Cambridge University Press, Cambridge.

[17] Knapp, A. W. (1986). *Representation Theory of Semisimple Groups: An Overview Based on Examples,* Princeton University Press, Princeton, NJ.

[18] Mallat, S. (1989). Multifrequency channel decomposition of images and wavelet models, *IEEE Trans. Acust., Speech, Signal Process.* **37**, 2091–2110.

[19] Mundy, J. L. and Zisserman, A., Eds., (1992). *Geometric Invariance in Computer Vision,* MIT Press.

[20] Potts, D., Steidl, G., and Tasche, M. (2000). Fast Fourier transform for nonequispaced data: A tutorial, in *Modern Sampling Theory: Mathematics and Applications*, 253–274, Benedetto, J. J. and Ferreira, P., Eds., Birkhäuser, Boston.

[21] Sally, P. J. Jr. (1976). Harmonic analysis and group representations, in *Studies in Harmonic Analysis,* Vol. 13, 224–256, Ash, J. M., Ed., MAA.

[22] Sandini, G., Questa, P., Scheffer, D., Dierickx, B., and Mannucci, A. (2000). A retina-like CMOS sensor and its applications, in *Proceedings of The 1st IEEE SAM Workshop,* held March 16-17, in Cambridge, (2000).

[23] Schwartz, E. L. (1977). Spacial mapping in primate sensory projection: Analytical structure and relevance to perception, *Biological Cybernetics* **25**, 181–194.

[24] Schwartz, E. L. (1994). Topographic mapping in primate visual cortex: History, anatomy, and computation, in *Visual Science and Engineering: Models and Applications,* Kelly, D. H., Ed., Marcel-Dekker.

[25] Shapiro, L. S. (1995). *Affine Analysis of Image Sequences,* Cambridge University Press, Cambridge.

[26] Turski, J. (1998). Harmonic analysis on $\mathbf{SL}(2, \mathbb{C})$ and projectively adapted pattern representation, *J. Fourier Anal. Appl.* **4**(1), 67–91.

[27] Turski, J. (1997). Projective Fourier analysis in computer vision: Theory and computer simulations, in *SPIE Vol. 3168, Vision Geometry VI,* 124–135. Malter, R. A., Wu, A. Y., and Latecki, L. J., Eds.

[28] Turski, J. (2000). Projective Fourier analysis for patterns, *Pattern Recognition* **33**, 2033–2043.

[29] Turski, J. (2001). Projective harmonic analysis and digital image processing, *The International Conference of Computational Harmonic Analysis,* held at City University of Hong Kong, June 4-8, (2001).

[30] Turski, J. (2003). Projective Fourier Analysis in computer vision: Mathematics for silicon retina of active vision sensors, *The 1st SIAM Conference: Mathematics for Industry—Challenges and Frontiers,* held in Toronto, Canada, October 13-15, (2003).

[31] Yeasin, M. (2001). Optical flow in log-mapped image plane—a new approach, *IEEE Trans. Pattern Analysis Mach. Intell.* **23**(11), 1–7.

Received September 18, 2003

Revision received February 24, 2004

Department of Computer and Mathematical Sciences, University of Houston-Downtown
e-mail: turskij@uhd.edu